AGU PUBLICATIONS

JGR

Journal of Geophysical Research: Atmospheres

RESEARCH ARTICLE
10.1002/2017JD026744

Key Points:
- Lightning discharges can influence the evolution of enhanced fluxes of energetic radiation and particles (TGEs)
- Only negative CGs and normal-polarity ICs were observed to abruptly terminate TGEs
- All TGEs occurred when the downward electron-accelerating electric field was present, at least for a portion of their duration

Correspondence to:
S. Soghomonyan,
surensog@gmail.com

Citation:
Chilingarian, A., Y. Khanikyants, E. Mareev, D. Pokhsraryan, V. A. Rakov, and S. Soghomonyan (2017), Types of lightning discharges that abruptly terminate enhanced fluxes of energetic radiation and particles observed at ground level, *J. Geophys. Res. Atmos.*, *122*, doi:10.1002/2017JD026744.

Received 2 MAR 2017
Accepted 11 JUL 2017
Accepted article online 15 JUL 2017

Types of lightning discharges that abruptly terminate enhanced fluxes of energetic radiation and particles observed at ground level

A. Chilingarian[1,2,3], Y. Khanikyants[1], E. Mareev[4], D. Pokhsraryan[1], V. A. Rakov[4,5], and S. Soghomonyan[1]

[1]Yerevan Physics Institute, Yerevan, Armenia, [2]National Research Nuclear University MEPhI (Moscow Engineering Physics Institute), Moscow, Russia, [3]Space Research Institute, RAS, Moscow, Russia, [4]Institute of Applied Physics, Russian Academy of Sciences, Nizhny Novgorod, Russia, [5]Department of Electrical and Computer Engineering, University of Florida, Gainesville, Florida, USA

Abstract We present ground-based measurements of thunderstorm-related enhancements of fluxes of energetic radiation and particles that are abruptly terminated by lightning discharges. All measurements were performed at an altitude of 3200 m above sea level on Mount Aragats (Armenia). Lightning signatures were recorded using a wideband electric field measuring system with a useful frequency bandwidth of 50 Hz to 12 MHz and network of five electric field mills, three of which were installed at the Aragats station, one at the Nor Amberd station (12.8 km from Aragats), and one at the Yerevan station (39 km from Aragats). We observed that the flux-enhancement termination was associated only with close (within 10 km or so of the particle detector) negative CGs and normal-polarity ICs; that is, with lightning types which reduce the upward directed electric field below the cloud and hence suppress the acceleration of electrons toward the ground.

1. Introduction

Thunderstorm Ground Enhancements (TGEs), i.e., enhanced fluxes of electrons, gamma rays, and neutrons detected by ground-based particle detectors during strong overhead thunderstorms and their abrupt termination by lightning discharges have been reported by several research groups [*Alexeenko et al.*, 2002; *Torii et al.*, 2011; *Tsuchiya et al.*, 2013; *Chilingarian et al.*, 2010, 2011; *Chilingarian et al.*, 2016].

However, some key questions on the origin of TGEs and their relation to lightning discharges still remain to be answered. Among the most important questions are the following: (1) what is the source of accelerating electric field responsible for TGE? (2) what types of lightning can terminate the TGE? (3) at what stage of lightning does the TGE termination occur?

The background flux of energetic radiation and particles at the Aragats station is about 400–600 counts/m^2/s for the plastic scintillators of 3 and 5 cm thick, depending on atmospheric pressure and energy threshold. Flux enhancements (TGEs) are not observed in fair weather; they occur (as the name suggests) only during thunderstorms and, as a rule, are accompanied by upward directed electrostatic field at the ground. Duration of TGE, including a rising part and a falling part, up to the terminating lightning event is 2–5 min. The maximum flux enhancement (TGE amplitude) observed to date at Aragats was 240% of the background (4 October 2014 at 14:12:15 UT). We usually measure the TGE amplitude in the number of standard deviations (from the background, measured before TGE) "contained" in the TGE maximum [*Chilingarian et al.*, 2015a, 2015b].

If the count rate enhancement in the 1 s time series reaches or exceeds 3 standard deviations (~15%), we accept the event as TGE. We verify our classification using data from other particle detectors installed at Aragats (detailed description of detectors and statistical analysis of TGE occurrences can be found in *Chilingarian et al.* [2013]. In 2008–2012, a total of 277 TGEs were observed at Aragats [*Chilingarian et al.*, 2013]; that is, about 55 per year (usually 1 to 3 per thunderstorm). The catalog of TGEs observed on Aragats in 2013–2016 is under preparation.

In order to gain insights into the physical mechanism of TGE termination by lightning, we examined measurements of electric field changes caused by lightning flashes that terminated the TGE. The measurements included the near-surface electrostatic field changes and "fast" wideband electric field waveforms. We also

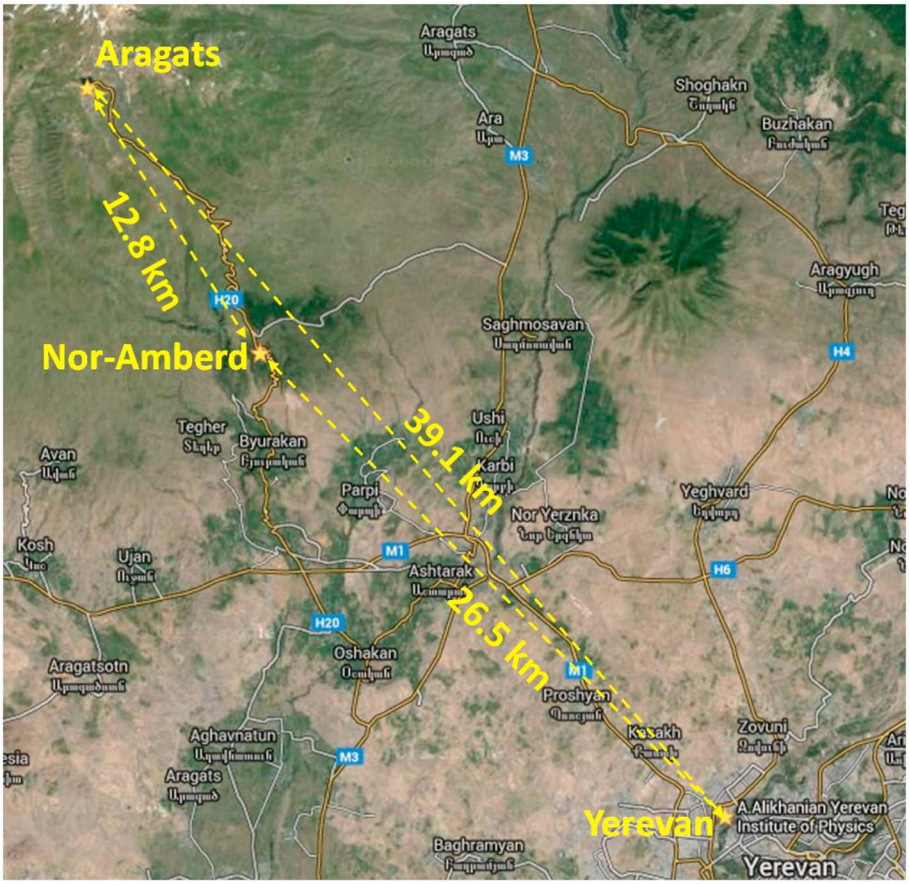

Figure 1. Locations of the Aragats, Nor Amberd, and Yerevan stations.

used lightning photography and data from the World Wide Lightning Location Network (WWLLN). This study is based on data acquired at the Aragats Space Environmental Center (ASEC) during the last five years (2012–2016). It is worth noting that gamma ray surges (glows) seen from balloons [*Eack et al*., 1996a, 1996b; *Eack and Beasley*, 2015] and aircraft [*Parks et al*., 1981; *McCarthy and Parks*, 1985; *Kelley et al*., 2015] are known to be often terminated by a lightning flash, but the type and characteristics of such terminating flashes are presently unknown.

The rest of the paper is organized as follows. In section 2, we briefly describe the instrumentation used in our study. In section 3, we explain the methodology used for lightning type identification. The data presentation, analysis, and discussion are divided into two parts: in section 4 we present examples of close lightning flashes of known types that were not associated with TGEs, and in section 5 we present 24 TGE-terminating lightning flashes, including their type and electric field signatures. The main results of the study are summarized in section 6.

2. Instrumentation

The data examined in this paper were acquired at the ASEC located at an altitude of 3200 m above sea level on Mount Aragats (Armenia). A 52 cm diameter circular flat-plate antenna was used to record the wideband (50 Hz to 12 MHz) electric field waveforms produced by lightning flashes.

The antenna was followed by a passive integrator (decay time constant = 3 ms); the output of which was connected via a 60 cm double-shielded coaxial cable to a Picoscope 5244B digitizing oscilloscope. The antenna calibration for electric field amplitude is presently not available, so the amplitude of recorded waveforms is given in voltage units of the oscilloscope. The oscilloscope was triggered by the signal from a commercial MFJ-1022 active whip antenna that covers a frequency range of 300 kHz to 200 MHz.

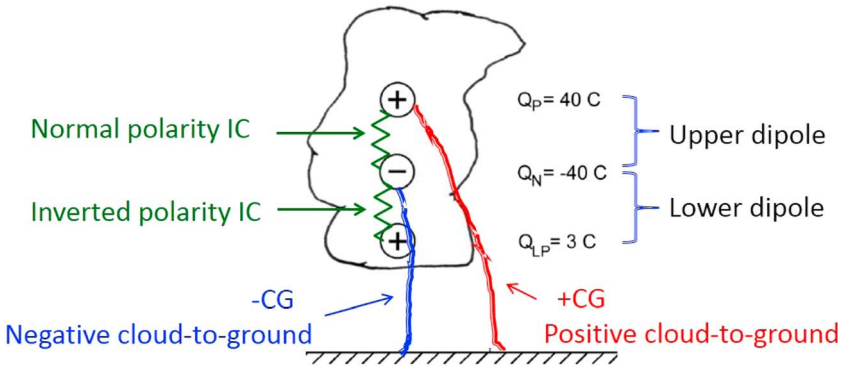

Figure 2. Schematic illustration of the "classical" tripolar charge structure of the thundercloud and four lightning types. Q_P = +40 C, Q_N = −40 C, and Q_{LP} = +3 C are typical thunderstorm cloud charges found in the literature, [e.g., *Rakov and Uman*, 2003, chapter 3]. The lower dipole is formed by Q_{LP} = 3 C and a portion of Q_N equal to −3 C.

The record length was 1 s including 200 ms pretrigger time and 800 ms posttrigger time. The sampling rate was 25 MS/s, corresponding to 40 ns sampling interval, and the amplitude resolution was 8 bit. The trigger-out pulse of the oscilloscope was relayed to the National Instruments (NI) myRIO board which produced the GPS time stamp of the record (detailed description of our fast data acquisition system based on the NI myRIO board can be found in *Pokhsraryan* [2015]). The flat-plate and the whip antennas were installed at the same location, within 80 m of particle detectors and two electric field mills. The distance from the antennas to third field mill was 270 m.

The near-surface electrostatic field changes were measured by a network of five field mills (Boltek EFM-100), three of which were placed at the Aragats station, one at the Nor Amberd station at a distance of 12.8 km from Aragats, and one at the Yerevan station, at a distance of 39.1 km from Aragats (Figure 1).

The distances between the three field mills at Aragats were 80 m, 270 m, and 290 m.

The electrostatic field changes were recorded at a sampling interval of 50 ms.

The TGEs analyzed in the present study were detected by an outdoor 3 cm thick scintillator with a sensitive area of 1 m^2. The detection efficiency is ~98% for electrons and ~2–3% for gamma rays, and the energy

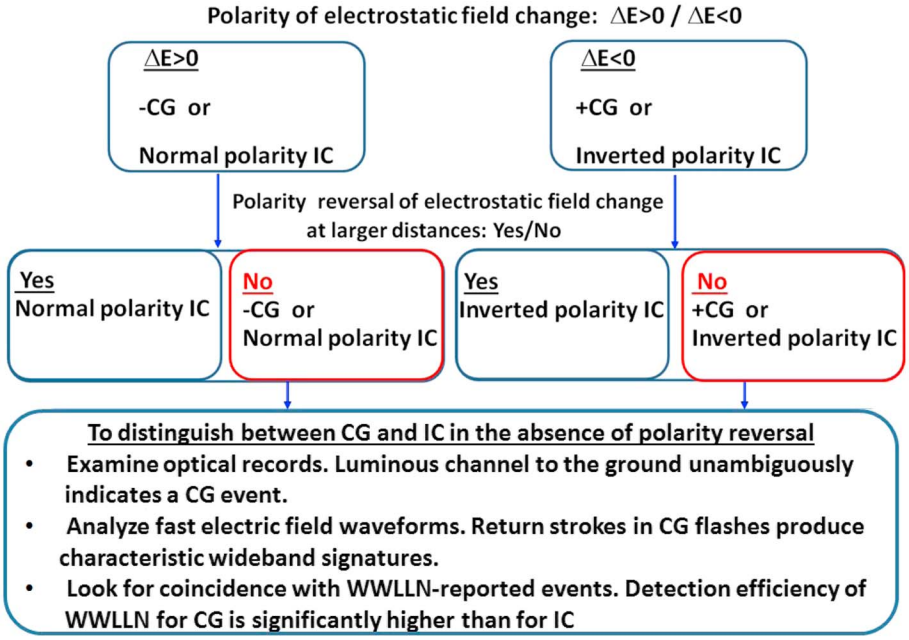

Figure 3. The algorithm of lightning type identification.

Table 1. Availability of ΔE Records, Wideband E Field Records, and WWLLN Data for 24 Lightning Events Terminating TGEs

Event ID	Date/Time (UTC)	ΔE (Number of Stations)	Wideband E Field Record	WWLLN Data	Lightning Type	Particle Flux Drop, %
1	7 Oct 2012, 15:10:53	4	No	No	-	22
2	12 May 2013, 06:37:52	3	No	No	-	20
3	19 Oct 2013, 11:20:53	4	No	Yes	−CG	58
4	26 May 2014, 13:12:41	3	No	No	-	13
5	2 Jun 2014, 21:00:11	3	No	No	-	24
6	2 Jun 2014, 20:58:10	3	No	No	-	22
7	4 Oct 2014, 14:13:32	3	Yes	No	−CG	32
8	20 Apr 2015, 18:02:01	4	Yes	No	+IC	25
9	20 Apr 2015, 18:00:14	4	Yes	Yes	+IC	91
10	11 May 2015, 16:29:36	4	Yes	Yes	−CG	24
11	11 May 2015, 16:32:06	4	Yes	Yes	−CG	70
12	11 May 2015, 16:35:06	4	Yes	Yes	−CG	44
13	7 Oct 2015, 14:45:07	4	Yes	No	+IC	22
14	28 Apr 2016, 18:23:02	4	Yes	No	+IC	9
15	28 Apr 2016, 18:24:38	4	Yes	Yes	+IC	8
16	4 May 2016, 19:04:33	4	Yes	Yes	−CG	20
17	4 May 2016, 19:05:58	4	Yes	No	+IC	14
18	10 May 2016, 14:15:48	4	Yes	No	+IC	23
19	10 May 2016, 14:17:46	4	Yes	No	+IC	13
20	4 Jun 2016, 01:25:24	4	Yes	No	+IC	20
21	11 Jun 2016, 11:45:23	4	Yes	Yes	+IC	11
22	16 Jun 2016, 10:02:11	4	Yes	No	+IC	14
23	16 Jun 2016, 10:05:13	4	Yes	No	+IC	12
24	28 Jul 2016, 13:56:34	4	Yes	No	−CG	19

threshold is ~2 MeV. The signals from the particle detectors, electric field meters, and flat-plate antenna were each GPS time stamped with relative timing accuracy of 1 ms. Lightning optical images were captured by a video camera at a frame rate of 30 frames per second. We also used data from the WWLLN, a global lightning location network which detects most intense very low frequency (VLF, 3–30 kHz) signals from lightning.

3. Methodology for Lightning-Type Identification

Lightning flashes can be grouped into two categories: those striking the ground and those not doing so. The intracloud to cloud-to-ground lightning flash ratio has been extensively studied in many regions all over the

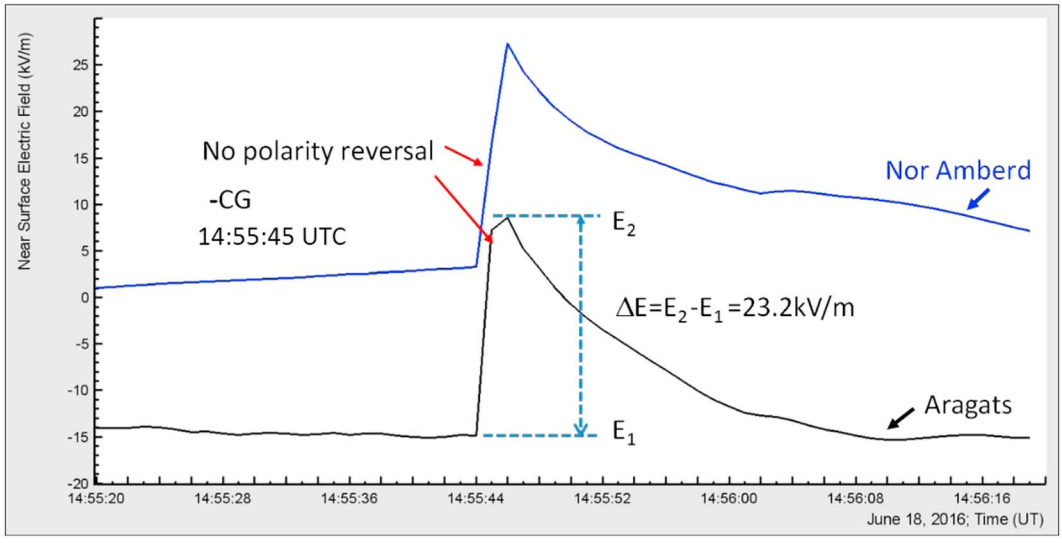

Figure 4. Electrostatic field changes produced by negative CG that occurred on 18 June 2016 at 14:55:45 UTC. The field changes are recorded by the field mills located in Aragats and Nor Amberd, separated by a distance of 12.8 km.

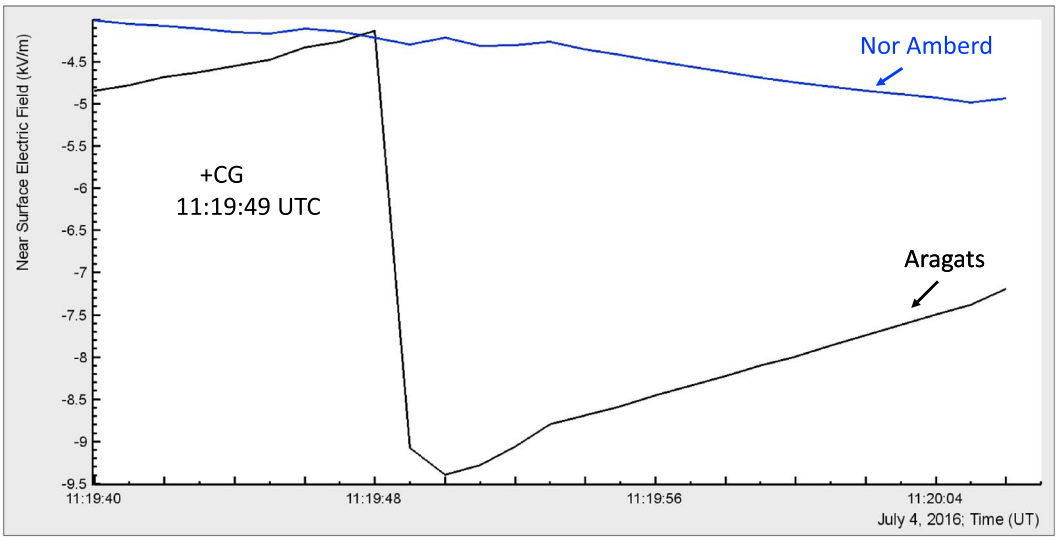

Figure 5. Electrostatic field changes produced by positive CG that occurred on 4 July 2016 at 11:19:49 UTC. The field changes are recorded by the field mills located in Aragats and Nor Amberd, separated by a distance of 12.8 km.

world [e.g., *Pierce*, 1970; *Prentice and Mackerras*, 1977; *MacGorman et al*., 1989; *Boccippio et al*., 2001; *Orville et al*., 2002; *Soriano and de Pablo*, 2007; *Kuleshov et al*., 2006; *de Souza et al*., 2009]. It is generally believed that intracloud, intercloud, and cloud-to-air flashes (all of which do not involve ground) comprise around 70–75% of lightning discharges, and that cloud-to-ground flashes comprise 25–30%.

The overwhelming majority of cloud-to-ground flashes transfer negative charge from the cloud to ground; they are called negative CGs. About 10% of ground flashes transfer positive charge to ground; they are referred to as positive CGs.

In our analysis we used the well-known vertical tripole model of the normal-polarity thundercloud charge structure. According to this model, there is a main negative charge region in the middle of the thundercloud, a main positive charge region at the top, and a much smaller positive charge near the cloud bottom. The latter is called the Lower Positive Charge Region (LPCR). It plays an important role in the initiation and development of lightning discharges. Different lightning scenarios that may arise depending upon the magnitude of the LPCR have been examined by *Nag and Rakov* [2009]. The LPCR usually serves as an igniting cell for initiating −CG and is largely consumed in the course of −CG. On the other hand, the presence of excessive LPCR may prevent the occurrence of a negative CG discharge and facilitate instead an intracloud (IC) discharge between the main negative charge region and the LPCR. Note that the normal-polarity IC flash occurs between the main negative and main positive charge regions, and that the IC flash between the main negative charge region and LPCR is sometimes referred to as the inverted-polarity IC. For our high-altitude experimental setup, the LPCR may be indistiguishable from the positive space charge produced by corona at ground level.

Four different lightning types are illustrated in Figure 2 by using the tripolar model of cloud charge structure. Negative cloud-to-ground (−CG) flash occurs between the main negative charge region and the ground. This lightning effectively transfers negative charge from the cloud to the ground. Positive cloud-to-ground (+CG) flash occurs between the main (upper) positive charge region and the ground and transfers a negative charge from the ground to the cloud (or, equivalently, positive charge from the cloud to the ground). Normal-polarity intracloud flash (+IC) occurs in the upper dipole between the main negative and main positive charge regions. Inverted-polarity intracloud flash (−IC) occurs in the lower dipole between the main negative charge region and the LPCR.

In this paper we use the atmospheric electricity sign convention, according to which the downward directed electric field or field change vector is considered to be positive. Electrons are accelerated downward to the ground by the upward directed electric field which is considered to be negative. Negative CG flashes serve to reduce the negative charge overhead, whereas normal-polarity IC flashes reduce (by equal amounts)

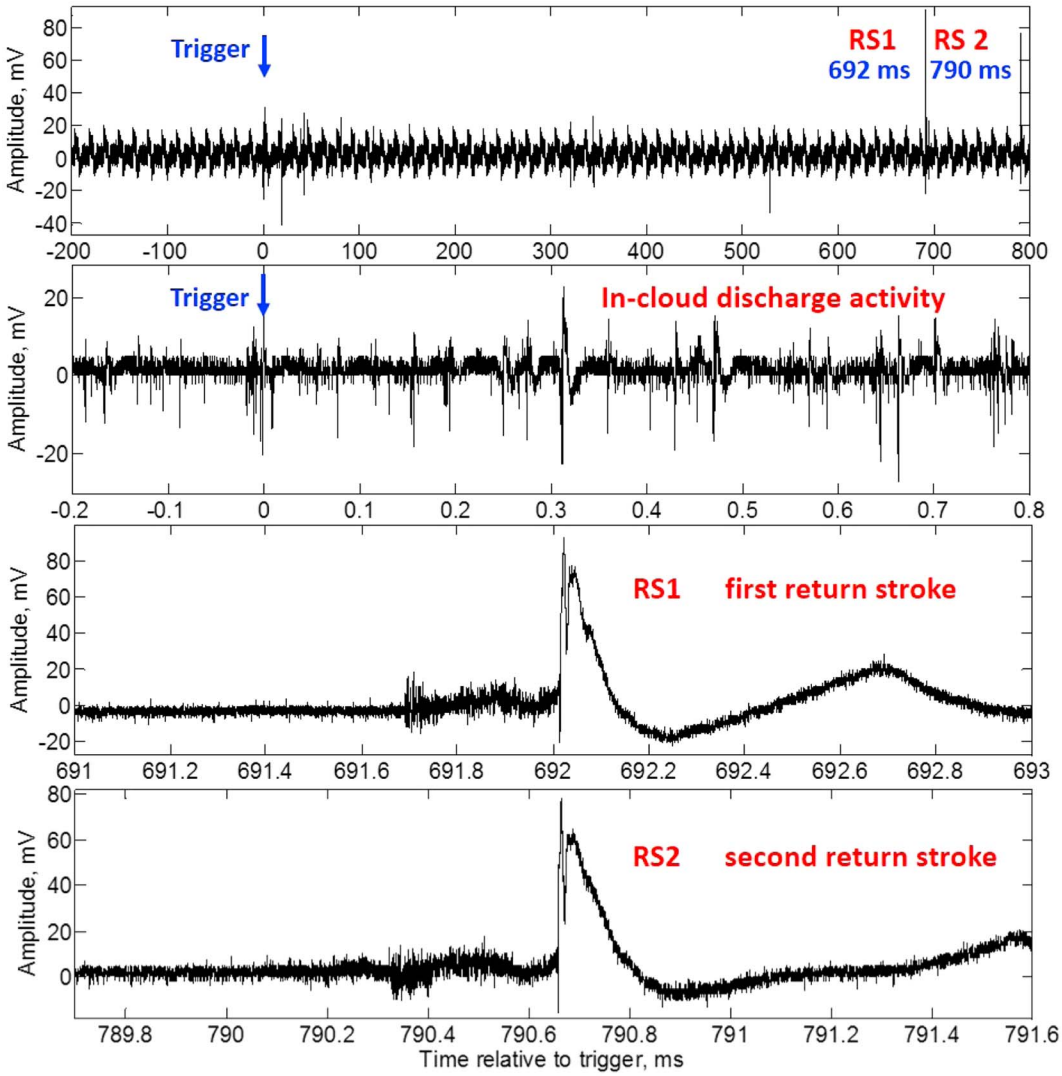

Figure 6. Fast electric field record of negative CG that occurred on 18 June 2016 at 14:55:45 UTC.

both the main negative and main positive charges overhead. At close distances, both of these lightning types produce electrostatic field changes of the same sign [*Rakov and Uman*, 2003, chapter 3; *MacGorman and Rust*, 1998, chapter 3]. This sign is positive according to the atmospheric electricity sign convention. Correspondingly, the positive CG and inverted-polarity IC flashes produce negative electric field changes at close distances. The polarity of electric field changes of CGs is independent of distance, while for IC flashes there is a polarity reversal distance.

The methodology of lightning type identification used in the present study is illustrated schematically in Figure 3. As mentioned above, our analysis is based on the tripolar model of the thundercloud charge structure resulting from normal electrification which is shown in Figure 2. First, we check the polarity of electrostatic field change at the Aragats station produced by the close lightning flash. If the field change is positive ($\Delta E > 0$), the flash is considered to be either $-$CG or normal-polarity IC. If the field change is negative ($\Delta E < 0$), the flash is considered to be either +CG or inverted-polarity IC.

Next, in order to distinguish between CGs and ICs, we check if the polarity of ΔE changes with distance, using our network of field mills. The polarity reversal is expected to occur at a distance of about 10 km for normal ICs and less than 5 km for inverted ICs [e.g., *Rakov and Uman*, 2003 chapters 3 and 4]. For a vertical dipole, the polarity of ΔE within the reversed distance is determined by the lower charge and beyond the reversal distance by the upper charge.

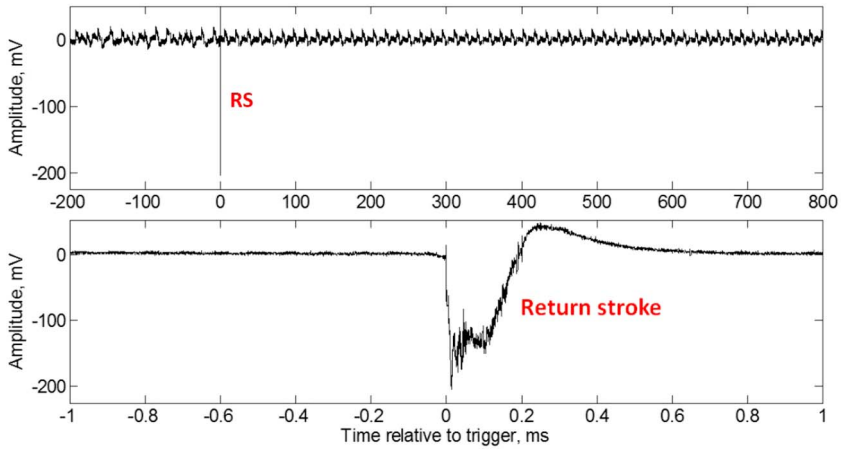

Figure 7. Fast electric field record of positive CG that occurred on 4 July 2016 at 11:19:49 UTC.

If polarity reversal has been detected, then we identify this lightning as a cloud discharge (normal-polarity or inverted-polarity IC). However, if polarity reversal has not been detected, the lightning-type identification question remains open, because the configuration of our field mill network (see Figure 1) was such that not all polarity reversals could be detected. In order to distinguish between cloud-to-ground and intracloud flashes in cases when the ΔE polarity reversal was not detected, we examined additional data. These additional data included lightning optical records, fast electric field waveforms, and WWLLN data (when available). Analysis of optical records is relatively simple: the image of luminous channel to the ground is indicative of a cloud-to-ground flash. Unfortunately, optical images were obtained only for two TGE-terminating lightning events (labeled 20 and 24 in Table 1). Fast electric field waveforms were used to search for characteristic return stroke (RS) signatures which are indicative of CGs. Needless to say that not every lightning event could be reliably classified using the methodology described above and illustrated in Figure 3.

In the analysis of fast electric field waveforms, the identification is accomplished by applying waveform criteria to individual electric field pulses. In most cases, RS signatures are readily identifiable in wideband *E* field record. Generally, bipolar, radiation-field pulses wider than certain threshold can be interpreted as being produced by return strokes in CG flashes, while narrower pulses are attributed to cloud flashes [*Zhu et al*., 2016].

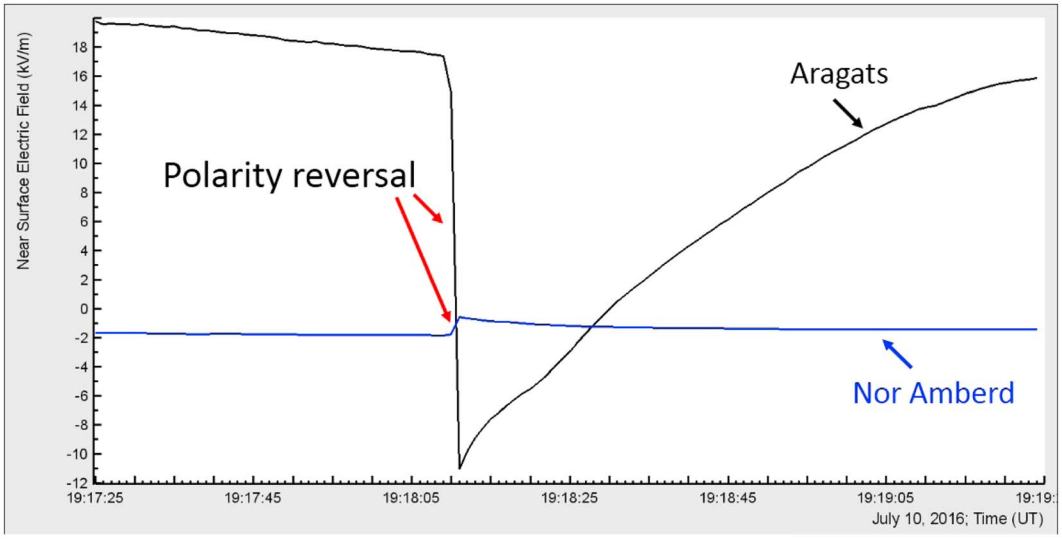

Figure 8. Electrostatic field changes of opposite polarity at Aragats and Nor Amberd, (separated by 12.8 km) produced by inverted-polarity IC flash that occurred on 10 July 2016 at 19:18:10 UTC.

Figure 9. Optical image of inverted-polarity IC flash on 10 July 2016 at 19:18:10 UTC.

For lightning classification and ranging purposes, we also looked for time coincidences of lightning events detected by our recording system with those found in the WWLLN database. It is generally believed that the detection efficiency of WWLLN for CGs is significantly higher than that for ICs [*Rodger et al.*, 2005]. Thus, if the flash in question is detected by the WWLLN, we assume that it is likely to be a CG flash.

4. Lightning Flashes Not Associated With TGEs

Not all close lightning flashes are accompanied by TGEs. TGE is a rather rare transient process whose occurrence depends on the presence of sufficiently high electric field region of sufficiently large vertical extent in the cloud directly above the particle detector(s) and the occurrence of sufficiently energetic electron in that region, as required for the onset and development of relativistic runaway electron avalanche (RREA) processes. It is the RREA processes in the in-cloud "accelerator" that are responsible for TGEs [*Chilingarian*, 2014]. Additionally, the emitting region should remain for several minutes above the particle detectors and close enough to the Earth's surface, so that the electron-gamma ray avalanche is not faded in the air. Clearly, lightning can occur when the in-cloud accelerator is not present or is not in a favorable position relative to detectors.

Examples of identified relatively close negative (at 9.2 km) and positive (at 13.1 km) cloud-to-ground lightning flashes not associated with TGEs are shown in Figures 4–7. Note that the distances have been estimated by one of the field mills and are approximate. Figures 4 and 5 show electrostatic field changes produced by those two lightning flashes detected in Aragats and Nor Amberd, separated by a distance of 12.8 km. No polarity reversal of the field change is observed for the lightning flash which occured at 14:55:45 (Figure 4) and for the flash at 11:19:49 (Figure 5). The polarity of electrostatic field change for the flash in Figure 4 is positive, and hence it can be either a negative cloud-to-ground flash (−CG) or a normal-polarity intracloud flash (+IC). There is no discernible ΔE signal at Nor Amberd in Figure 5, and, hence, no polarity reversal can be detected for this event. Thus, the lightning-type identification question remains open. The polarity of electrostatic field change for the flash in Figure 5 is negative, and hence, it can be either a positive cloud-to-ground flash (+CG) or an inverted-polarity intracloud flash (−IC). Definition of the electrostatic field change ΔE produced by lightning is illustrated, for the Aragats record, in Figure 4.

We additionally analyzed fast electric field waveforms of these lightning flashes, which are shown in Figures 6 and 7. The record in Figure 6 contains a relatively long sequence of smaller pulses characteristic of in-cloud discharge activity followed by two strong and relatively wide pulses of positive polarity at 692 ms and 790 ms after the trigger. The risetime of these two pulses is about 7–8 μs, and the peak-to-zero fall time is 100–110 μs. The positive initial polarity of these two essentially radiation (judging from the waveforms) pulses is the same as the polarity of electrostatic field changes shown in Figure 4. With a high level of confidence we attribute

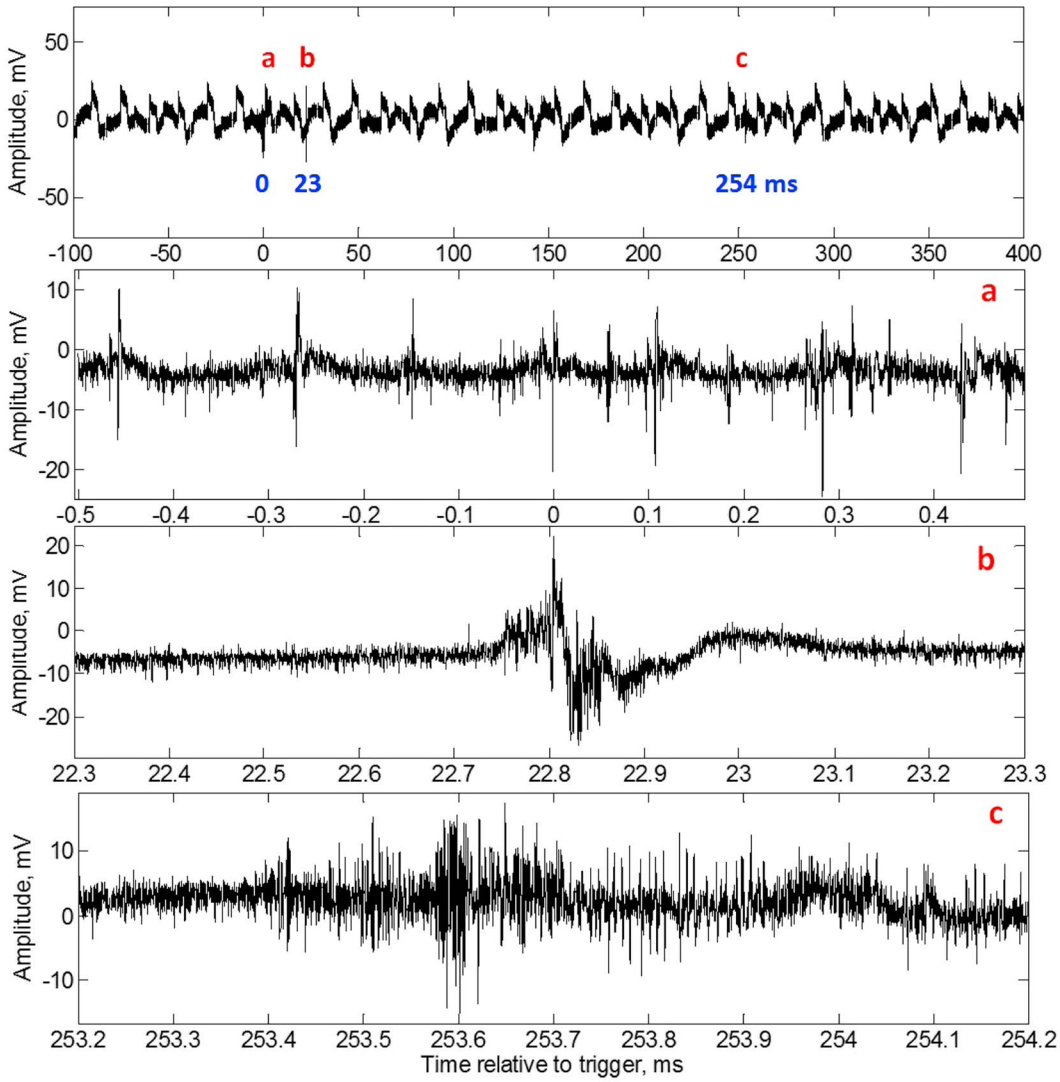

Figure 10. Fast electric field record of inverted-polarity IC flash that occurred on 10 July 2016 at 19:18:10 UTC.

these two pulses to return strokes of negative cloud-to-ground (−CG) lightning. The noise in Figure 6 (upper panel) is caused by the 50 Hz electromagnetic interference (distorted due to 3 ms decay time constant of the antenna integrator).

The record in Figure 7 does not contain any pronounced pulses indicative of in-cloud discharge activity, only a single large pulse which has a 10 μs risetime and a peak-to-zero fall time of 180 μs. The initial polarity of this pulse is the same as that of the electrostatic field changes shown in Figure 5. We classify this pulse as the return stroke pulse of positive cloud-to-ground (+CG) lightning.

An example of inverted-polarity intracloud flash is presented in Figures 8–10, which show electrostatic field changes produced by this lightning (Figure 8), single frame of optical record (Figure 9), and fast electric field record (Figure 10).

As can be seen from Figure 8, the electrostatic field changes detected by two field mills in Aragats and Nor Amberd have opposite polarities, that is, polarity reversal with distance is detected. Therefore, this lightning can be identified as an intracloud flash, because, as mentioned earlier, the polarity reversal with distance occurs only when an elevated dipole is neutralized. This classification is supported by the corresponding optical image shown in Figure 9, which clearly shows that there is no luminous channel to the ground. The polarity of the larger field change detected in Aragats corresponds to a closer distance and is negative, which is

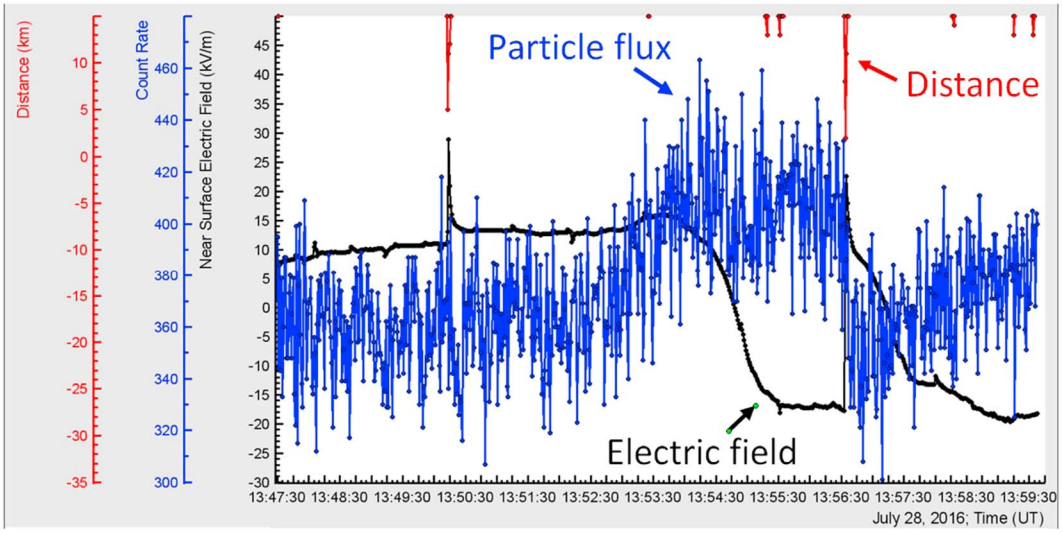

Figure 11. Electrostatic field change and particle flux (count rate, count per second) detected at Aragats for TGE (about 20% above the background) terminated by lightning flash (28 July 2016, 13:56:34 UTC). Distance to lightning from the particle detector estimated by one of the field mills at Aragats is indicated in red.

indicative of inverted-polarity intracloud flash. Identification of this event as a cloud flash is further supported by the fast electric field record (see Figure 10) which contains only short bipolar pulses of microsecond and submicrosecond duration and no signatures characteristic of return strokes.

5. Lightning Flashes That Terminated the TGE

In this section we will consider 24 lightning flashes, each of which appeared to have terminated the TGE. In Table 1, we show the availability of various records for 24 lightning events that terminated TGEs. Lightning types (when identified) and associated particle flux drops (as percentages relative to background) are also given.

An example of TGE abruptly terminated by lightning flash is presented in Figure 11. The black curve shows the electrostatic field measured by electric field mill at Aragats, the blue curve shows radiation and particle

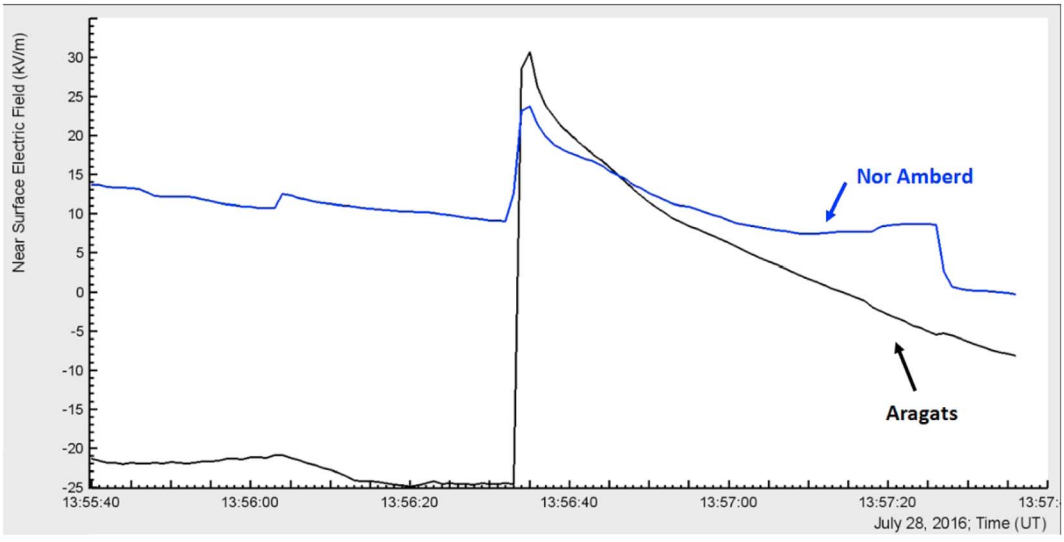

Figure 12. Electrostatic field changes recorded by the field mills in Aragats and Nor Amberd for TGE-terminating lightning flash (28 July 2016, 13:56:34 UTC) shown in Figure 9.

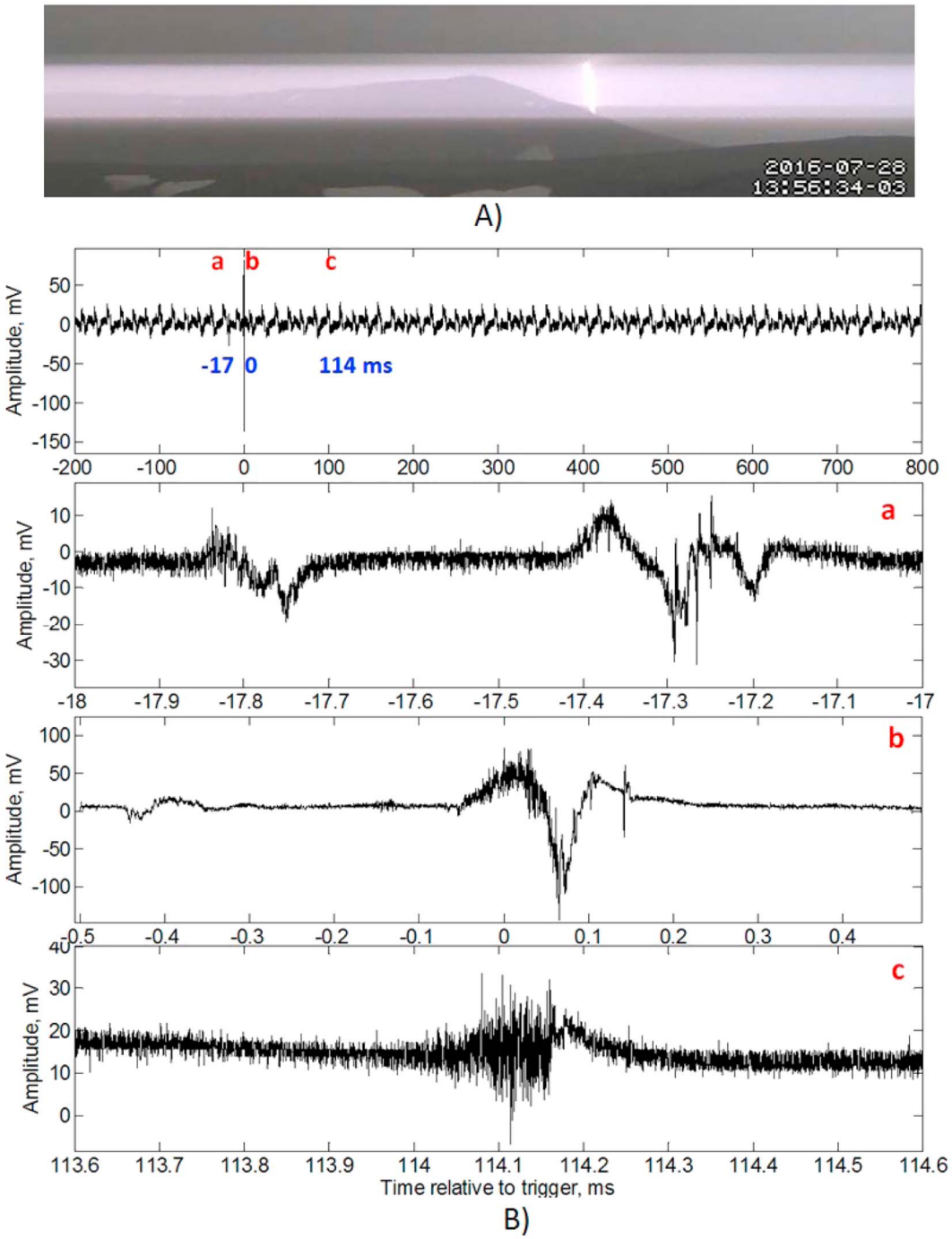

Figure 13. (A) Optical and (B) fast electric field records corresponding to lightning flash that terminated the TGE on 28 July 2016 at 13:56:34 UTC (see also Figures 11 and 12).

flux measured by scintillation detector (1 s time series), and the red lines denote the distance to lightning from the detector site.

As mentioned above, the negative upward directed electrostatic field accelerates electrons downward to the ground and initiates an electron avalanche multiplication and gamma rays. This accelerating field can be formed by the main negative charge of the thundercloud and its mirror image in the ground. Inside the thundercloud, this field can be enhanced by the LPCR located below the main negative charge region. The fast change of the electrostatic field sign caused by the lightning discharge leads to abrupt termination of the

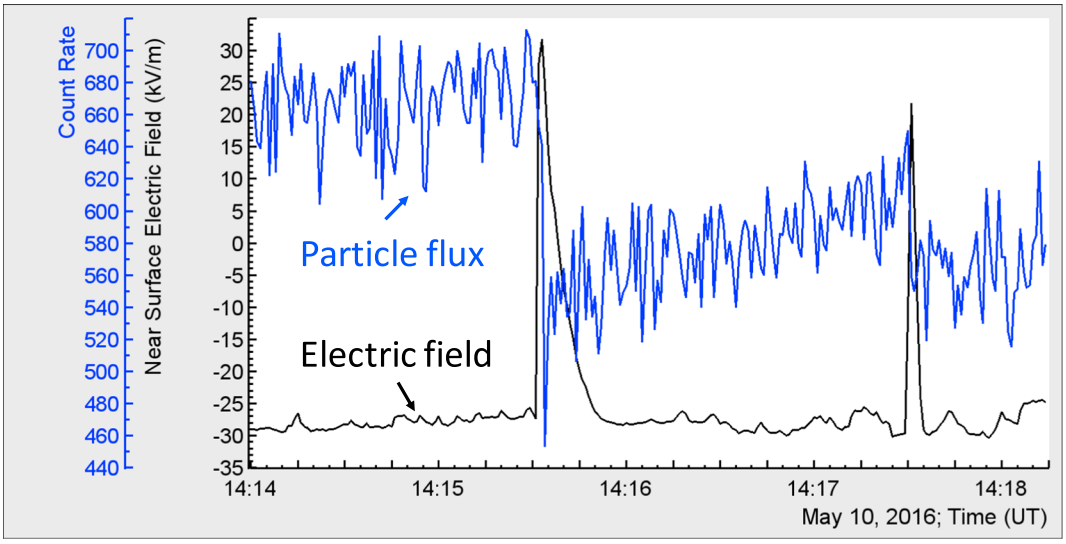

Figure 14. Electrostatic field change and particle flux (count rate, count per second) measured at Aragats for a sequence of two TGEs, each terminated by a lightning flash (10 May 2016, (left) 14:15:48 UTC and (right) 14:17:46 UTC).

TGE. The fast positive change of electrostatic field can be associated with negative CG that serves to reduce the main negative charge of the thundercloud. Alternatively, it could be a normal-polarity IC, which is shown not to be the case below.

Note that the TGE shown in Figure 11 begins during a period when the electrostatic field is in the positive domain. One possible reason for this behavior is that at the start of "summer" TGEs, when the cloud bases are higher compared to spring and autumn TGEs, the radiation region in the bottom of thundercloud starts to illuminate the detector site before the cloud positions itself above the detectors. Thus, we can speculate that low-energy Compton scattered gamma rays from the RREA cascades unleashed in the thundercloud can reach the detectors even when the electric field is in the positive domain. For the event shown in Figure 11, the field starts declining soon after the beginning of TGE and rapidly moves to the negative domain.

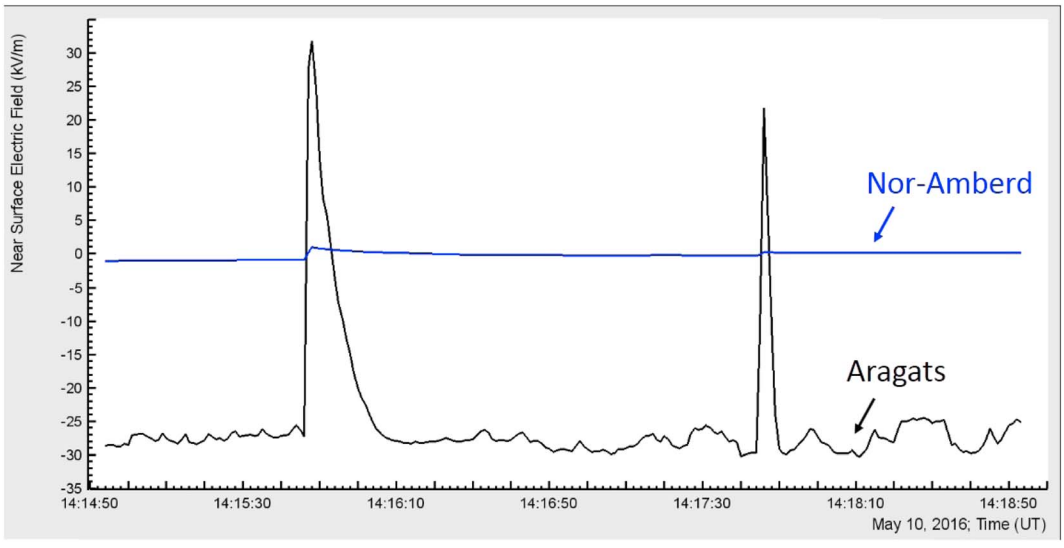

Figure 15. Electrostatic field changes recorded by field mills in Aragats and Nor Amberd for a sequence of two TGEs, each terminated by a lightning flash (10 May 2016, (left) 14:15:48 and (right) 14:17:46).

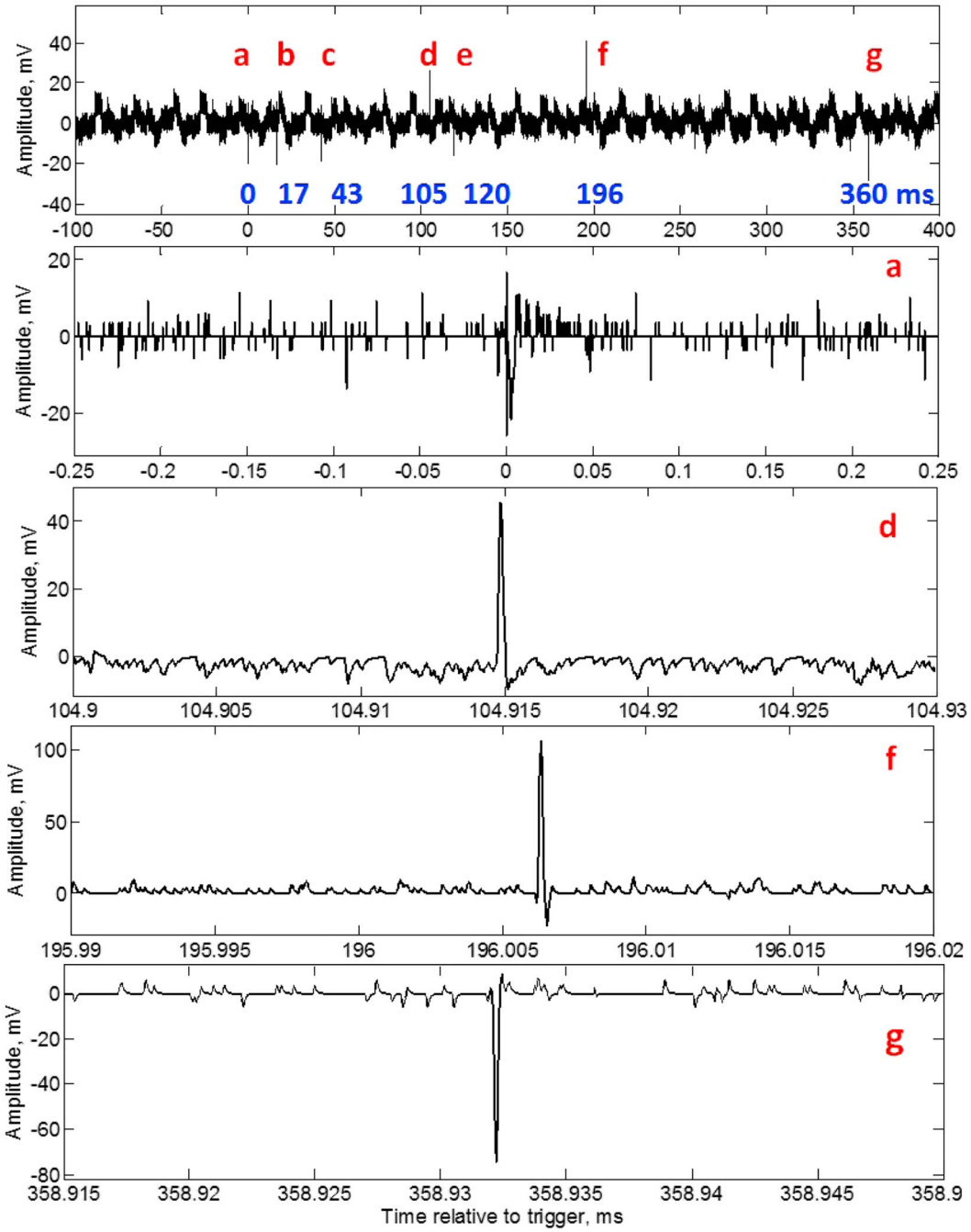

Figure 16. Fast electric field record of lightning flash that occurred on 10 May 2016 at 14:15:48 UTC and terminated the earlier of the two TGEs shown in Figures 14 and 15. Pulses labeled b, c, and e in the top panel are similar to pulse a and are not shown on an expanded time scale.

Figure 12 shows electrostatic field changes recorded by field mills in Aragats and Nor Amberd. Distance to lightning estimated by EFM-100 field mill is about 2 km from Aragats and about 10 km from Nor Amberd. This lightning event has been also detected by the WWLLN. It can be seen from Figure 12 that both field mills detected positive field change. The absence of polarity reversal suggests that this lightning is a negative cloud-to-ground (−CG) flash, as opposed to a normal-polarity intracloud flash.

We additionally analyzed our optical and fast electric field records corresponding to the lightning event that occurred on 28 July 2016, 13:56:34 UTC. Those records are shown in Figure 13. Lightning channel in Figure 13

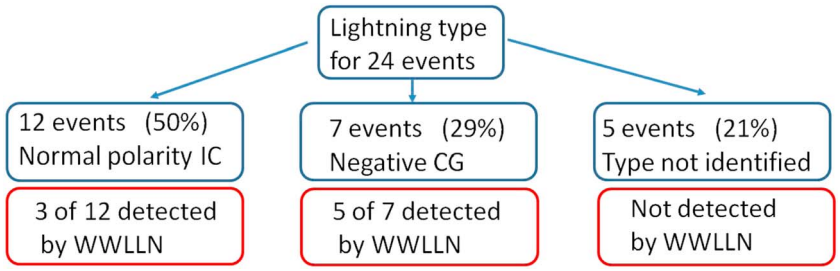

Figure 17. Types of lightning flashes that terminated TGEs.

A clearly terminates on the ground, strongly supporting our classification of this lightning as cloud-to-ground flash. On the other hand, no waveform characteristic of return stroke is found in the fast *E* field record shown in Figure 13B.

A sequence of two TGEs, each terminated by lightning flash, is presented in Figure 14 which shows 1 s time series of particle flux (upper blue curve) and electrostatic field (lower black curve). Two abrupt changes of electrostatic field produced by nearby lightning flashes are accompanied by abrupt decreases of particle flux.

Note that after the fast change of electrostatic field caused by the first flash at 14:15:48 the field returns during several seconds to the preceding level of −30 kV/m. The monotonically increasing particle count between the two flashes can be associated with this strong negative electric field which should accelerate electrons toward to the ground**.** Similar behavior can be seen after the second termination of the particle flux at 14:17:46, when the field returns to its preceding negative value, and the particle count rate tends to increase again. The recovered strong negative field after each of the two lightning flashes on a time scale of a few seconds indicates that the intense electrification processes continued in the cloud.

Figure 15 shows the electrostatic field changes for these two lightning flashes that were recorded in Aragats and Nor Amberd. It is seen from Figure 15 that both field changes are positive, which suggests that the lightning events were either negative cloud-to-ground (−CG) flashes or normal-polarity intracloud flashes.

In order to distinguish between these two lightning types we examined the corresponding fast electric field record shown in Figure 16. No optical record for this event is available.

As seen in Figure 16, there are only very short pulses with durations less than 1 μs. The fast field record of the second flash (14:17:46 UTC), not shown here, is similar. There are no pulses that could be attributed to return strokes of cloud-to-ground lightning. Based on the entirety of information available, we identify these two lightning events as normal-polarity intracloud flashes.

Classification of lightning flashes for 24 TGEs that were terminated by lightning is summarized in Figure 17. Nearly 50% of the TGE-terminating lightning events have been identified as normal-polarity intracloud flashes, and a quarter of them (3 out of 12) have been detected by WWLLN. About 29% of the events have been identified as negative cloud-to-ground flashes, and about 70% of them (five out of seven) have been detected by WWLLN. About 21% of the events (five events observed in 2012–2014; see Table 1) for which no optical or wideband electric field records were available and which were not detected by the WWLLN were classified as not identified.

In Table 2, we compare the distances to lightning from particle detectors estimated by electric field mill EFM-100 at Aragats and those obtained from the WWLLN data.

Table 2. Distances (kilometers) Estimated by Electric Field Mill EFM-100 and WWLLN for Eight Lightning Events That Terminated TGEs

Event ID in Table 1	10	11	12	9	3	15	16	21	Mean ± Standard Deviation
EFM-100	4	7.9	2.9	2.0	11	7.1	6.2	2.2	5.4 ± 3.2
WWLLN	0.6	13.7	4.2	6.7	4.9	6.0	0.9	6.2	5.4 ± 4.1

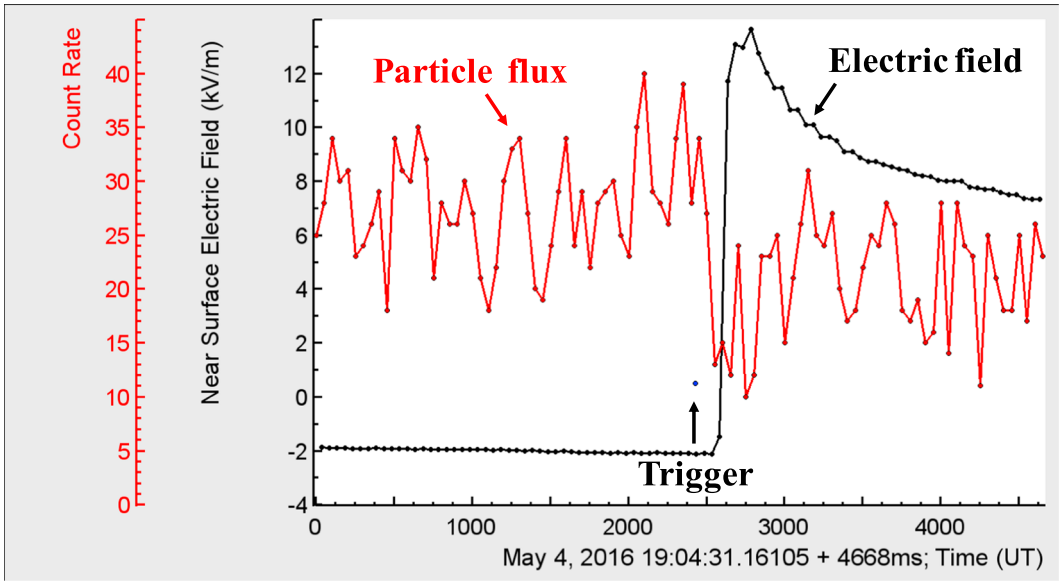

Figure 18. Electrostatic field and particle flux (count rate, count per 50 ms) for the TGE terminated by lightning flash that occurred on 4 May 2016 at 19:04:33 UTC. The GPS time stamp of the oscilloscope trigger assumed to be a proxy for the start of significant electromagnetic emission from lightning discharge is indicated by vertical arrow, labeled "Trigger."

It appears from Table 2 that, regardless of the source of data (WWLLN or EFM-100), all the distances are within ~10 km of the particle detector, with only one exception (event 11). The mean values for both EFM-100 and WWLLN are about 5 km.

It follows from Figure 17 that both negative cloud-to-ground and normal-polarity intracloud flashes can terminate TGEs. We emphasize that at close distances both types of lightning produce net positive changes of electrostatic field resulting from the reduction of negative charge overhead. This corresponds to the reduction of upward directed (electron-accelerating) electric field below the cloud.

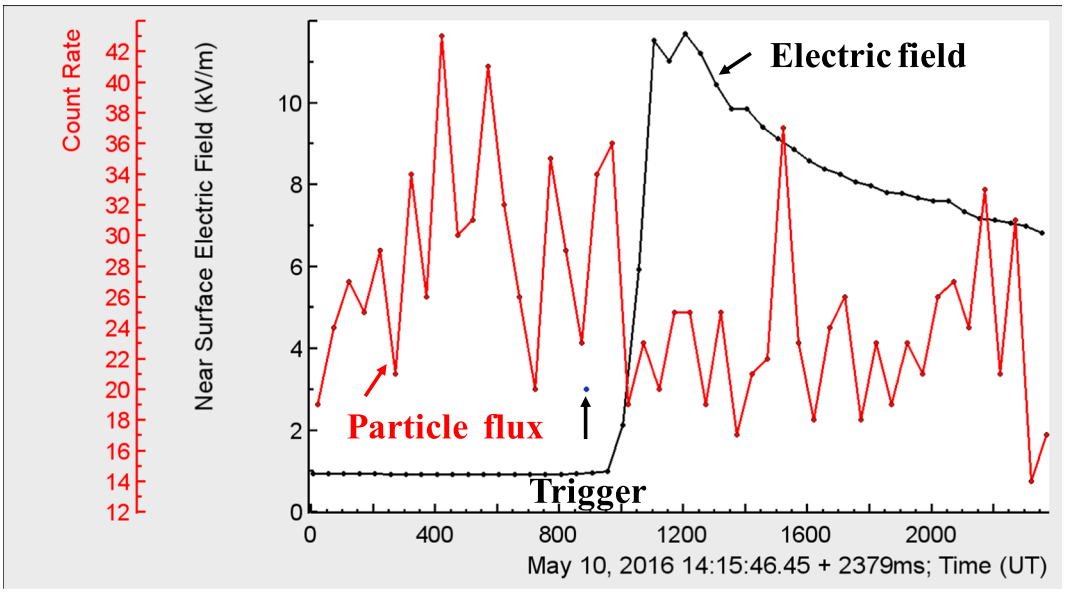

Figure 19. Electrostatic field and particle flux (count rate, count per 50 ms) for the TGE terminated by lightning flash that occurred on 10 May 2016 at 14:15:48 UTC. The GPS time stamp of the oscilloscope trigger assumed to be a proxy for the start of significant electromagnetic emission from lightning discharge is indicated by vertical arrow.

Table 3. Beginning of the Count Rate Decrease Relative to Trigger

Event ID in Table 1	16	17	18	19	20	21	23	24	Mean ± Standard Deviation
Time (ms)	104	313	31	225	235	67	215	266	182 ± 101

To gain an insight into the temporal evolution of TGE termination by lightning flash, we have analyzed the relative timing of (1) the start of electromagnetic emission from lightning discharge detected using the whip antenna; see section 2, (2) the start of particle flux decay, and (3) the maximum of electrostatic field change on a millisecond time scale. Two examples of such analysis are presented in Figures 18 and 19, which show 50 ms time series of particle flux and electric field, along with the trigger time of the wideband electric field measuring system.

The start of significant electromagnetic emission from lightning was assumed to correspond to the trigger time of the digital oscilloscope, which recorded the fast wideband electric field waveforms. As mentioned in section 2, the oscilloscope was triggered by the signal from the antenna operating in the 300 kHz to 200 MHz range (covering the MF, HF, and part of VHF ranges), and the trigger was GPS time stamped. The trigger time is indicated by vertical arrow in each Figures 18 and 19.

For the TGE shown in Figure 18, the electromagnetic emission starts at t_1 = 19:04:33.592, whereas the maximum of electrostatic field change is attained at t_2 = 19:04:33.800; that is, 208 ms later. It can be seen from the figure that the decay of particle flux starts in the time interval between the time instants t_1 and t_2. Uncertainties in the determination of the trigger position and of the maximum of electrostatic field change are about 1 ms and 10 ms, respectively.

Similar relative timing is observed for another event, as shown in Figure 19. The electromagnetic emission starts at 14:15:47.337; maximum of electrostatic field change is attained at 14:15:47.772, that is, 435 ms later; and the decay of particle flux starts in the time interval between these two instants. Such analysis could be performed for a total of nine TGEs terminated by lightning and showed that the time interval between the start of electromagnetic emission and the maximum of electrostatic field change produced by lightning ranged from 210 ms to 360 ms, with average value of 284 ms and standard deviation of 45 ms.

To find the beginning of the count rate decrease, we used Student's *t* test and a sliding window approach. The algorithm looks for the point in 50 ms time series, for which the *t* test value is maximum for two groups of the sample, one before and the other after this point (the regime change point). In Table 3, we present the results obtained with a 300 ms sliding window for eight out of the nine analyzed events. These results show that the time interval between the trigger and the beginning of the count rate decrease is in the range from 31 ms to 313 ms. For one of the nine events we could not reliably identify the beginning of the count rate decrease due to large fluctuations in the count rate data.

Parameters of electrostatic field changes and associated particle flux drops for 24 analyzed events are presented in Table 4.

The magnitude of electric field change is defined as the difference between the maximum of electrostatic field and its value just prior to the beginning of abrupt change, as illustrated in Figure 4.

It is important to note that we did not observe any TGE termination by lightning which produced a negative field change; that is, for all TGEs terminated by lightning, the field change was positive. As noted earlier, positive field changes reduce the upward directed electric field, accelerating electrons toward ground, which leads to a decrease of particle count rate.

Table 4. Parameters of Electrostatic Field Changes and Associated Particle Flux Drops for 24 TGEs Terminated by Lightning

Parameter	Mean ± Standard Deviation
Rise time of electrostatic field (ms)	217 ± 82
Recovery time of electrostatic field (full width at half maximum) (s)	5.5 ± 4.7
Magnitude of electric field change (kV/m)	61 ± 16
Distance to lightning estimated by EFM-100 (km)	5.6 ± 3.0
Particle flux (count rate) drop (%)	29 ± 23

6. Conclusions

Main results of the present study are summarized below. Note that in our analysis we assumed the "classical" vertical tripole model of the cloud charge structure.

1. The downward electron-accelerating electric field can be formed by the main negative charge in the cloud and its mirror image in the ground. This field is influenced by other charges in the cloud (and their images) and can be locally enhanced by the LPCR in the cloud and positive corona space charge near the ground. All TGEs observed at Aragats occurred when the downward electron-accelerating electric field was present at the ground, at least for a portion of their duration.
2. The electric field both inside and beneath the thundercloud can be abruptly changed by lightning discharges, which can influence the evolution of TGEs, including their abrupt termination.
3. Two types of flashes were observed to terminate TGEs, namely, −CGs and normal-polarity ICs. Both these types reduce the main negative charge in the cloud. Normal-polarity ICs also reduce the main positive charge, but reduction of lower negative charge has the dominant effect.
4. Neither +CGs nor inverted-polarity ICs were observed during TGEs. The latter type does reduce the main negative charge in the cloud, but its net effect is to enhance the downward electron-accelerating field below the cloud due to the accompanying reduction or elimination of LPCR. We do not expect +CG or inverted-polarity ICs to terminate TGEs, but further research is needed to confirm this.
5. The decay of particle flux begins in the time interval between the start of significant wideband electromagnetic emission from the lightning discharge and the maximum of electrostatic field change produced by the discharge.
6. Not every TGE-terminating lightning could be reliably classified using the lightning-type identification scheme used in the present study. In a follow-up study we plan to improve the classification accuracy via better optical coverage of the detected events and the use of better instrumentation for measuring wideband *E* field waveforms. We also plan to improve the lightning ranging accuracy. Those improvements should allow us to, among other things, estimate the percentages of each type of lightning both terminating and not terminating TGEs.

Acknowledgments
The authors would like to thank the staff of the Aragats Space Environmental Center for the uninterruptible operation of Aragats research station facilities. The data for this paper are available via the multivariate visualization software ADEI on the Web page of the Cosmic Ray Division (CRD) of the Yerevan Physics Institute http://adei.crd.yerphi.am/adei. The expedition to Aragats high-altitude station was supported by the Armenian Government grant N13-1C275. This work was also supported in part by the Ministry of Education and Science of the Russian Federation (project 14. B25.31.0023).

References

Alexeenko, V. V., N. S. Khaerdinov, A. S. Lidvansky, and V. B. Petkov (2002), Transient variations of secondary cosmic rays due to atmospheric electric field and evidence for pre-lightning particle acceleration, *Phys. Lett. A*, *301*, 299–306.

Boccippio, D. J., K. L. Cummins, H. J. Christian, and S. J. Goodman (2001), Combined satellite- and surface-based estimation of the intracloud-cloud-to- ground lightning ratio over the continental United States, *Mon. Weather Rev.*, *129*, 108–129.

Chilingarian, A., A. Daryan, K. Arakelyan, A. Hovhannisyan, B. Mailyan, L. Melkumyan, G. Hovsepyan, S. Chilingaryan, A. Reymers, and L. Vanyan (2010), Ground-based observations of thunderstorm-correlated fluxes of high-energy electrons, gamma rays, and neutrons, *Phys. Rev. D*, *82*, 043009.

Chilingarian, A., G. Hovsepyan, and A. Hovhannisyan (2011), Particle bursts from thunderclouds: Natural particle accelerators above our heads, *Phys. Rev. D: Part. Fields*, *83*(6), 062001.

Chilingarian, A., T. Karapetyan, and L. Melkumyan (2013), Statistical analysis of the thunderstorm ground enhancements (TGEs) detected on Mt. Aragats, *J. Adv. Space Res.*, *52*, 1178.

Chilingarian, A. (2014), Thunderstorm ground enhancements—Model and relation to lightning flashes, *J. Atmos. Sol. Terr. Phys.*, *107*, 68–76.

Chilingarian, A., S. Chilingaryan, and G. Hovsepyan (2015a), Calibration of particle detectors for secondary cosmic rays using gamma-ray beams from thunderclouds, *Astropart. Phys.*, *69*, 37–43.

Chilingarian, A., G. Hovsepyan, Y. Khanikyanc, A. Reymers, and S. Soghomonyan (2015b), Lightning origination and thunderstorm ground enhancements terminated by the lightning flash, *Europhys. Lett.*, *110*, 49001.

Chilingarian, A., G. Hovsepyan, and E. Mnatsakanyan (2016), Mount Aragats as a stable electron accelerator for atmospheric high-energy physics research, *Phys. Rev. D*, *93*, 052006.

de Souza, P. E., O. Pinto, I. R. C. A. Pinto, N. J. Ferreira, and A. F. dos Santos (2009), The intracloud/cloud-to-ground lightning ratio in south-eastern Brazil, *Atmos. Res.*, *91*, 491–499.

Eack, K. B., and W. H. Beasley (2015), Long-duration X-ray emissions observed in thunderstorms, *J. Geophys. Res. Atmos.*, *120*, 6887–6897, doi:10.1002/2015JD023262.

Eack, K. B., W. H. Beasley, W. D. Rust, T. C. Marshall, and M. Stolzenburg (1996a), Initial results from simultaneous observations of X rays and electric fields in a thunderstorm, *J. Geophys. Res.*, *101*, 29,637–29,640, doi:10.1029/96JD01705.

Eack, K. B., W. H. Beasley, W. D. Rust, T. C. Marshall, and M. Stolzenburg (1996b), X-ray pulses observed above a mesoscale convective system, *Geophys. Res. Lett.*, *23*, 2915–2918.

Kelley, N. A., et al. (2015), Relativistic electron avalanches as a thunderstorm discharge competing with lightning, *Nat. Commun.*, *6*, 7845.

Kuleshov, Y., D. Mackerras, and M. Darveniza (2006), Spatial distribution and frequency of lightning activity and lightning flash density maps for Australia, *J. Geophys. Res.*, *111*, D19105, doi:10.1029/2005JD006982.

MacGorman, D. R., and W. D. Rust (1998), *The Electrical Nature of Thunderstorms*, 422 pp., Oxford Univ. Press, New York.

MacGorman, D. R., D. W. Burgess, V. Mazur, W. D. Rust, W. L. Taylor, and B. C. Johnson (1989), Lightning rates relative to tornadic storm evolution on 22 May 1981, *J. Atmos. Sci.*, *46*, 221–250.

McCarthy, M., and G. K. Parks (1985), Further observations of X-rays inside thunderstorms, *Geophys. Res. Lett.*, *12*, 393–396, doi:10.1029/GL012i006p00393.
Nag, A., and V. Rakov (2009), Some inferences on the role of lower positive charge region in facilitating different types of lightning, *Geophys. Res. Lett.*, *36*, L05815, doi:10.1029/2008GL036783.
Orville, R. E., G. R. Huffines, W. R. Burrows, R. L. Holle, and K. L. Cummins (2002), The North American Lightning Detection Network (NALDN)-first results: 1998–2000, *Mon. Weather Rev.*, *130*, 2098–2109.
Parks, G. K., B. H. Mauk, R. Spiger, and J. Chin (1981), X-ray enhancements detected during thunderstorm and lightning activities, *Geophys. Res. Lett.*, *8*, 1176–1179.
Pierce, E. T. (1970), Latitudinal variation of lightning parameters, *J. Appl. Meteorol.*, *9*, 194–195.
Pokhsraryan D. (2015), Fast data acquisition system based on NI-myRIO board with GPS time stamping capabilities for atmospheric electricity research, in *Proceedings of TEPA 2015*, pp. 23–27, Nor Amberd, Tigran Mets.
Prentice, S. S., and D. Mackerras (1977), The ratio of cloud to cloud-ground lightning flashes in thunderstorms, *J. Appl. Meteorol.*, *16*, 545–549.
Rakov, V. A., and M. A. Uman (2003), *Lightning: Physics and Effects*, Cambridge Univ. Press, New York.
Rodger, C. J., J. B. Brundell, and R. L. Dowden (2005), Location accuracy of VLF World-Wide Lightning Location (WWLL) network: Post-algorithm upgrade, *Ann. Geophys.*, *23*, 277–290.
Soriano, L. R., and F. de Pablo (2007), Total flash density and the intracloud/cloud-to-ground lightning ratio over the Iberian Peninsula, *J. Geophys. Res.*, *112*, D13114, doi:10.1029/2006JD007624.
Torii, T., et al. (2011), Migrating source of energetic radiation generated by thunderstorm activity, *Geophys. Res. Lett.*, *38*, L24801, doi:10.1029/2011GL049731.
Tsuchiya, H., et al. (2013), Detection of high-energy gamma rays from winter thunderclouds, *Phys. Rev. Lett.*, *111*, 015001.
Zhu Y., V. Rakov, M. Tran, and A. Nag (2016), A study of NLDN responses to cloud discharge activity based on ground-truth data acquired at the LOG, *24th International Lightning Detection Conference and 6th International Lightning Meteorology Conference*, San Diego, Calif., 18–21 April.